

# Modelling and Nonlinear Analysis of Journal Center Trajectory of Sleeve Bearing with Different Axial Oil Grooves

Lili Wang\*, Min Wang\*\*, Yuliang Wei\*\*\*, Xue Ge\*\*\*and Wei Zhang\*\*\*

**Keywords:** sleeve bearing, axial oil grooves, dynamic loading model, journal center trajectory.

## ABSTRACT

Based on the motion equation of journal center trajectory, the nonlinear journal center trajectory under dynamic load is calculated, and the journal center trajectory of cylindrical bearing, two-axial groove journal bearing and three-axial groove journal bearing is compared. When dynamic load is applied in bearing, the journal center oscillates and adjusts again, and finally stabilizes at a new balanced position. The more the number of oil grooves is, the faster the sleeve bearing journal center velocity tends to be stable. The three-axial groove journal bearing has the fastest stabilizing speed, the advantage of good impact resistance and stability; the cylindrical bearing have the slowest stabilizing speed, the worst impact resistance and stability.

## INTRODUCTION

In the application process of journal bearings, due to various operating conditions, the process of forming and stabilizing for the oil film of journal bearing is different. The study of the nonlinear journal center trajectory is helpful to simulate the working state of journal bearing, which is of great significance for the structural optimization and operating conditions of journal bearing.

*Paper Received June, 2021. Revised January, 2022. Accepted March, 2022. Author for Correspondence: Lili Wang, Min Wang.*

\* Associate Professor, College of Mechanical and Electronic Engineering, Shandong University of Science and Technology, Qingdao, 266590, China.

\*\* Associate Professor, College of Mechanical and Electronic Engineering, China university of Petroleum, Qingdao 266580, China.

\*\*\* Graduate Student, College of Mechanical and Electronic Engineering, Shandong University of Science and Technology, Qingdao, 266590, China.

Meng et al. (2008) solved the Reynolds equation by successive over-relaxation method (SOR method) on the basis of finite difference method, obtains the width-diameter ratio and eccentricity on oil film distribution curve of oil film pressure of journal bearing, and studied the influence of bearing the basis pressure distribution. Joy et al. (2016) studied the static characteristics of two-axial groove journal bearing with different groove structures, and optimized the groove structure of two-axial groove journal bearing by genetic algorithm. Ma et al. (2010) calculated the journal center trajectory, maximum oil film pressure and minimum oil film thickness of journal bearing under step loads, rectangular pulse loads and sinusoidal impulse loads, and summarized their change rules. Sharma et al. (2017) obtained the influence of surface roughness on bearing stability by calculating the journal center trajectory. Jain et al. (2017) analyzed the linear and nonlinear transient motion of the two-lobe journal bearing, by comparing with the journal center trajectory of the circular bearing, it was concluded that the two-lobe journal bearing is more stable than the circular bearing. Lin et al. (2014) analyzing the transient nonlinear motion. Li et al. (2015) calculated the static equilibrium position under different static loads, bearing structures, oil film clearances and journal rotational speeds, and concluded that the static equilibrium position of journal center trajectory was independent of the initial position of journal. Ye et al. (2016) studied the journal orbit and circumferential pressure distribution of journal bearing by experimental method, and analyzed the influence of the clearance radius, the aspect ratio and the rotational speed on the bearing stability. Li (1999) has analyzed the journal center orbits based on a non-isothermal non-Newtonian fluid model, and studied the influence of the journal rotation speed and the frequency of change of the applied load on the stability of journal bearing. Dong et al. (2017) analyzed the influence of surface texture distribution on vibration and stability of bearing by experiment. Cha et al. (2013) studied the influence of unbalanced

force, load, eccentricity and other factors on the journal orbit by comparing the journal trajectories obtained by the linear and nonlinear transient analysis. Mehrjardi et al. (2016) studied the effect of preload factor on the stability performance of noncircular two and three lobe journal bearings by analyzing the linear and nonlinear journal orbit. Hakan et al. (2013) studied the tribological properties of non-grooved and micro-grooved journal bearings under dynamic loading by comparing the experimental and numerical results.

By solving the generalized Reynolds equation and the force balance equation, Wang et al. (2018) obtained that the circumferential pressure, axis displacement, axis velocity, axis acceleration velocity of journal bearing change periodically as time goes, and the influence of dynamical loading on the oil film pressure distribution and the journal center trajectory is analyzed. Tatsuya et al. (2017) made a nonlinear theoretical analysis of a flexible rotor system supported by a full circle bearings, and studied the influence of various parameters on the lubrication performance of journal bearings. Conti et al. (2016) have studied a new quasi-3D tilting pad journal bearing model, which can analyze both the fluid dynamics and rotor dynamics of the system and their complex interactions. Sunnegård et al. (2016) studied how the cross-coupling coefficients affected the dynamics of a vertical rotor with tilting pad journal bearings, it was found that the cross-coupling stiffness for vertical machines can influence the dynamics by compared the simulated unbalanced response with the experimental results. Zhou et al. (2017) conducted an experimental study on the water film pressure of water-lubricated rubber bearings with multiple grooves, and concluded that the water-lubricated rubber bearings with multiple grooves have a significant influence on the film pressure circumferential distribution. Wang et al. (2020) studied the accurate nonlinear dynamic characteristics of the gas journal bearings. Hekmat et al. (2019) indicated that the presence of the groove in the bearings caused the pressure on the grooved bearings to decrease dramatically, and the probability of occurrence of the oil instability will be less than no groove bearing.

Most scholars have focused on the static characteristics or stiffness damping coefficients of journal bearing, and neglected the influence of oil groove structure on journal center trajectory. The research on journal center trajectory is more helpful to simulate the state of journal bearing under the actual working condition, and makes the research result more close to the actual situation, the study of oil groove structure is helpful for improving the stability of spindle system. Therefore, the manuscript mainly studies and analyzes the journal orbit of sleeve bearings with different oil groove structures.

## ESTABLISHMENT OF THEORETICAL MODEL

### Oil Film Thickness Equation of Different Oil Grooves at Dynamic Loading

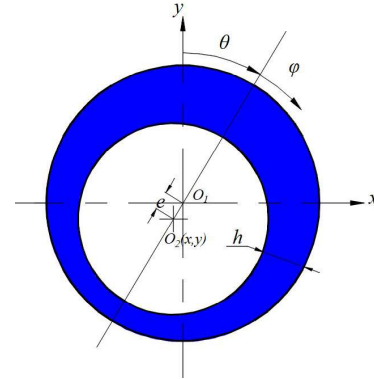
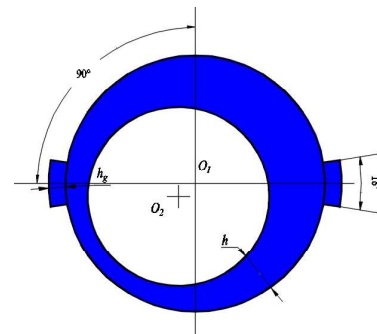
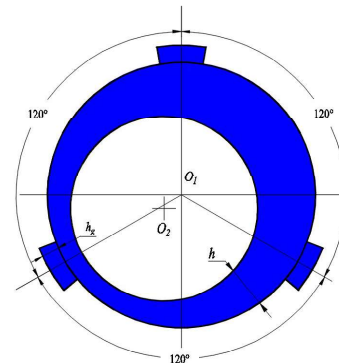


Fig. 1. Geometrical structure of sleeve bearing.



(a) Two-axial groove bearing



(b) Three-axial groove bearing

Fig. 2. Geometrical structure of groove bearing

As shown in Figure 1,  $O_1$  is bearing center,  $O_2$  is denoted by  $(x, y)$  and it is axis center,  $O_1O_2$  is eccentricity, a wedge-shaped gap is formed between the bearing bush and the axis due to the existence of eccentricity  $e$ ,  $\theta$  is attitude angle,  $\phi$  is circumferential angle and begins at the maximum oil film thickness, the oil film thickness equation of cylindrical bearing is shown as:

$$h = c + e \cos \phi \quad (1)$$

where  $h$  is the oil film thickness,  $c$  is the radial clearance.

In Fig. 1, when the coordinates of the axis  $O_2$  is represented by  $(x, y)$ , the parameters can be expressed as follows (Ma et al., 2010; Zhang, 1986):

$$\begin{aligned} e &= \sqrt{x^2 + y^2} \\ \sin \theta &= x / e \\ \cos \theta &= y / e \end{aligned}$$

The film thickness equation (1) can be expressed as:

$$h = c + x \sin(\varphi + \theta) + y \cos(\varphi + \theta) \quad (2)$$

The dimensionless form of equation (2) can be expressed as:

$$H = 1 + X \sin(\varphi + \theta) + Y \cos(\varphi + \theta) \quad (3)$$

where  $H$  is the non-dimensional oil film thickness,  $H = \frac{h}{c}$ ,  $X$  and  $Y$  are the non-dimensional displacement of the journal center in the  $x$  direction and  $y$  direction.

Similarly, as shown in Figure 2, the oil film thickness equation of the oil grooves is

$$h = c + x \sin(\varphi + \theta) + y \cos(\varphi + \theta) + h_g \quad (4)$$

where  $h_g$  is the depth of the oil groove.

The dimensionless form of equation (4) is

$$H = 1 + X \sin(\varphi + \theta) + Y \cos(\varphi + \theta) + H_g \quad (5)$$

where  $H_g$  is the non-dimensional depth of oil groove,

$$H_g = \frac{h_g}{c}.$$

### Reynolds equation

The Reynolds equation for incompressible fluid lubrication and finite long bearing can be expressed as (Zhang, 1986):

$$\frac{\partial}{\partial x} \left( h^3 \frac{\partial p}{\partial x} \right) + \frac{\partial}{\partial y} \left( h^3 \frac{\partial p}{\partial y} \right) = 6U\mu \frac{\partial h}{\partial x} \quad (6)$$

where  $p$  is the oil film pressure,  $U$  is journal rotation speed,  $\mu$  is lubricating oil viscosity.

For the oil groove sleeve bearing, the oil film thickness of bearing has a stepped change, the Reynolds equation contains the derivative of  $h$ , and it cannot be directly transformed into a difference equation at the oil groove position. Therefore, it is necessary to use the flow balance relationship in the limited control space ( $2 \Delta x \times 2 \Delta y$ ) to solve the discontinuous position of the oil film thickness.

$$\begin{aligned} & \frac{\Delta y}{2} \left[ \frac{Uh_{i-1,j+0}}{2} - \frac{h_{i-1,j+0}^3}{12\mu} \frac{p_{i,j} - p_{i-1,j}}{\Delta x / 2} \right] + \frac{\Delta y}{2} \left[ \frac{Uh_{i-1,j-0}}{2} - \frac{h_{i-1,j-0}^3}{12\mu} \frac{p_{i,j} - p_{i-1,j}}{\Delta x / 2} \right] \\ & + \frac{\Delta x}{2} \left[ \frac{h_{i+0,j-1}^3}{12\mu} \frac{p_{i,j-1} - p_{i,j}}{\Delta z / 2} \right] + \frac{\Delta x}{2} \left[ \frac{h_{i-0,j-1}^3}{12\mu} \frac{p_{i,j-1} - p_{i,j}}{\Delta z / 2} \right] \\ & + \frac{\Delta y}{2} \left[ \frac{Uh_{i+1,j-0}}{2} - \frac{h_{i+1,j-0}^3}{12\mu} \frac{p_{i+1,j} - p_{i,j}}{\Delta x / 2} \right] + \frac{\Delta y}{2} \left[ \frac{Uh_{i+1,j+0}}{2} - \frac{h_{i+1,j+0}^3}{12\mu} \frac{p_{i+1,j} - p_{i,j}}{\Delta x / 2} \right] \\ & + \frac{\Delta x}{2} \left[ \frac{h_{i-0,j+1}^3}{12\mu} \frac{p_{i,j} - p_{i,j+1}}{\Delta z / 2} \right] + \frac{\Delta x}{2} \left[ \frac{h_{i+0,j+1}^3}{12\mu} \frac{p_{i,j} - p_{i,j+1}}{\Delta z / 2} \right] = 0 \end{aligned} \quad (7)$$

where  $i+0$ ,  $i-0$  denote the oil film thickness near

the column  $i$  in the positive and negative direction of the  $x$ -axis, separately,  $j+0$ ,  $j-0$  is similar for column  $j$  and  $y$ -axis.

The dimensionless component of the oil film forces in the direction of  $x$  and  $y$  are as follows:

$$\begin{aligned} F_x &= - \int_0^{2\pi} \left( \int_{-1}^1 P d\lambda \right) \sin(\varphi + \theta) d\varphi \\ F_y &= - \int_0^{2\pi} \left( \int_{-1}^1 P d\lambda \right) \cos(\varphi + \theta) d\varphi \quad (8) \\ W &= \sqrt{F_x^2 + F_y^2} \quad (9) \end{aligned}$$

where  $F_x$  and  $F_y$  are the dimensionless component of the oil film forces in the direction of  $x$  and  $y$ ,  $W$  is the non-dimensional loading capacity.

### Nonlinear motion equation of journal center trajectory

As shown in Fig. 1, the motion equation of the journal center  $O_2$  in the coordinate system  $xO_1y$  is

$$ma_x = f_x(\omega t) + q_x \quad (10)$$

$$ma_y = f_y(\omega t) + q_y + mg \quad (11)$$

where  $m$  is the quality of shaft,  $a_x$  and  $a_y$  are the accelerations in the direction of  $x$  and  $y$ ,  $\omega$  is the rotational speed of sleeve bearing,  $t$  is the time,  $f_x(\omega t)$  and  $f_y(\omega t)$  indicate the component of the oil film force in the direction of  $x$  and  $y$  at the speed  $\omega$  and time  $t$ ,  $q_x$  and  $q_y$  are the dynamic loads acting on the rotation axis in the  $x$  and  $y$  directions.

The equation (10) and (11) are divided by  $mc\omega^2$  and obtained the dimensionless form as follows:

$$A_x = k_m F_x(\tau) + Q_x \quad (12)$$

$$A_y = k_m F_y(\tau) + Q_y + j_m \quad (13)$$

where

$$A_x = \frac{a_x}{c\omega^2}, A_y = \frac{a_y}{c\omega^2}, k_m = \frac{\mu l}{m\omega} \left( \frac{r}{c} \right)^3, \tau = \omega t, j_m = \frac{g}{c\omega},$$

$$F_x = f_x \left/ \mu \omega r l \left( \frac{r}{c} \right)^2 \right., F_y = f_y \left/ \mu \omega r l \left( \frac{r}{c} \right)^2 \right., Q_x = \frac{q_x}{mc\omega},$$

$$Q_y = \frac{q_y}{mc\omega}, \quad r \text{ is bearing radius.}$$

### Calculation of nonlinear center trajectory of journal bearing

#### Calculation method of nonlinear center trajectory of journal bearing

The boundary conditions adopt the Reynolds boundary condition. Pressure at both edges of the bearing is zero. Pressure distribution is symmetric about the mid plane along axial direction. When the pressure falls below zero, the oil film rupture occurs, the Reynolds boundary condition on the rupture

boundary is used, pressure and pressure gradient is set equal to 0.

In order to solve the nonlinear center trajectory of journal bearing, the film thickness equation (equations (3) and (5)) of the initial position should be solved, and then the Reynolds equation can be solved. The Reynolds equation of cylindrical bearing (equation (6)) is solved by finite difference method because of its simple bearing structure (Zhang, 1986). The Reynolds equation of journal bearing with groove is mainly solved by the flow conservation relationship in the control space (equation (7)).

The distribution of oil film pressure can be obtained by solving Reynolds equation, and then the components of oil film pressure  $F_x$  and  $F_y$  can be calculated according to equation (8). The accelerations of journal center  $A_x$  and  $A_y$  can be obtained by substituting  $F_x$  and  $F_y$  into equation of motion (12) and (13). By Euler method, the displacement and velocity at the next moment of the journal center  $O_2$  can be calculated. The new displacements are substituted into the film thickness equation and the next iteration is carried out. Finally, the nonlinear journal center trajectory is obtained.

#### Basic calculation parameters of journal bearing

The basic parameters of bearing calculation are as follows:

Table 1. Bearing calculation parameter (Ma et al., 2010; Wang et al., 2018; Zhang, 1986).

Bearing parameters	Notations	Numerical value
length of the bearing (m)	$l$	0.05
Journal radius (m)	$r$	0.025
radial clearance (m)	$c$	0.0002
rotor quality(Kg)	$m$	10
viscosity of lubricating oil(Pa·s)	$\mu$	0.02
Journal rotational speed(rad/s)	$\omega$	$100\pi$

In the following calculation, the starting point of the nonlinear journal trajectory is selected as the center point of the bearing. The time range  $\tau$  is 0 to  $30\pi$ , and  $\Delta\tau$  is  $\pi/100$ . The non-dimensional depth of the oil groove  $H_g$  is 1, and the groove width is 18 degrees, the structure is shown in Fig. 2; the oil grooves of the two-axial groove journal bearing are located on the horizontal line of the bearing with an interval of 180 degrees, and the oil grooves of three-axial groove journal bearing are located on the bearing with an interval of 120 degrees.

#### Results and discussion

$$Q_x = \begin{cases} 0 & 0 \leq \tau < 15\pi \\ 1 & 15\pi \leq \tau \leq 30\pi \end{cases}$$

$$Q_y = \begin{cases} 0 & 0 \leq \tau < 15\pi \\ 1 & 15\pi \leq \tau \leq 30\pi \end{cases} \quad (14)$$

When journal bearing is in the state of dynamic load as shown in equation (14), the journal center trajectory, journal center displacement, journal center velocity, journal center acceleration and oil film pressure distribution of the journal bearing are as shown in Figure. 3, 4, 5, and 6.

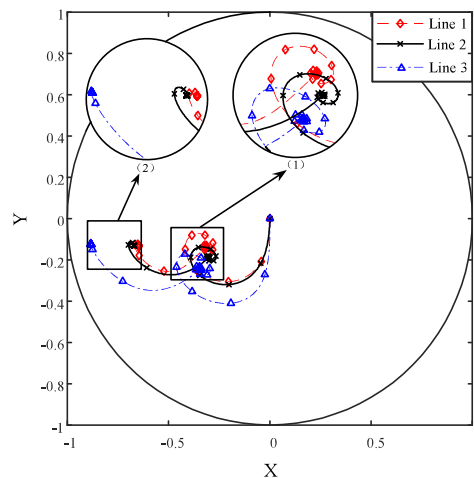


Fig. 3. Journal center trajectory under dynamic load (Line 1 represents the journal center trajectory of cylindrical bearing; Line 2 represents the journal center trajectory of two-axial groove journal bearing; Line 3 represents the journal center trajectory of three-axial groove journal bearing.)

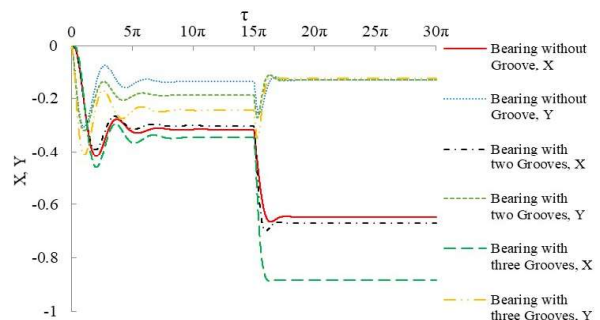
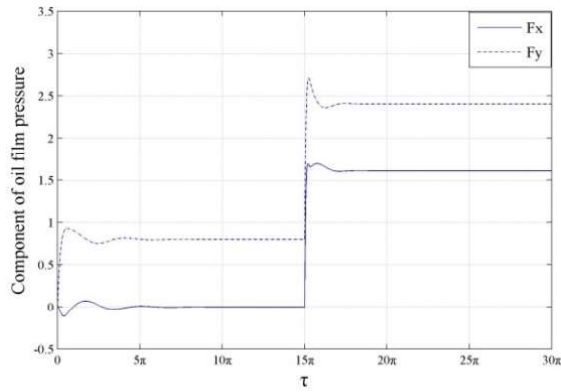
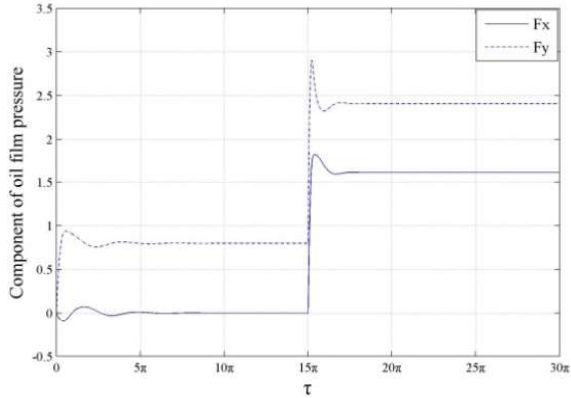


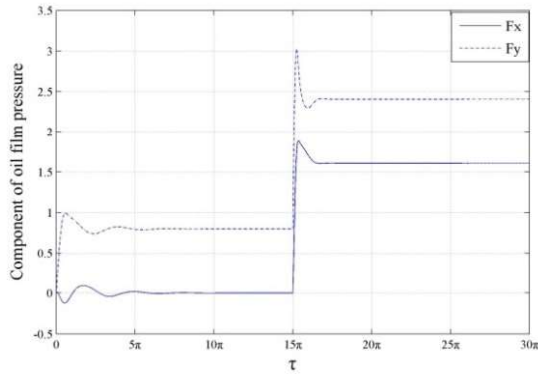
Fig. 4 Journal center displacement under dynamic load



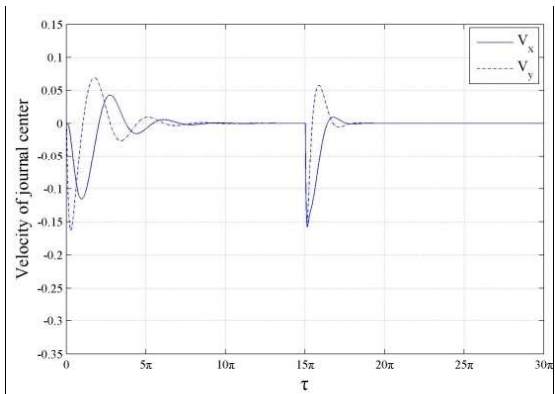
(a) Oil film components of cylindrical bearing



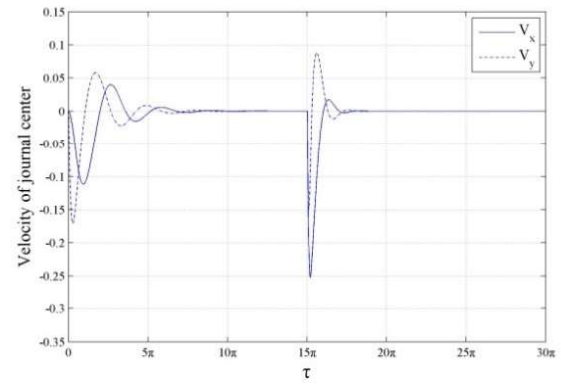
(b) Oil film components of two-axial groove bearing



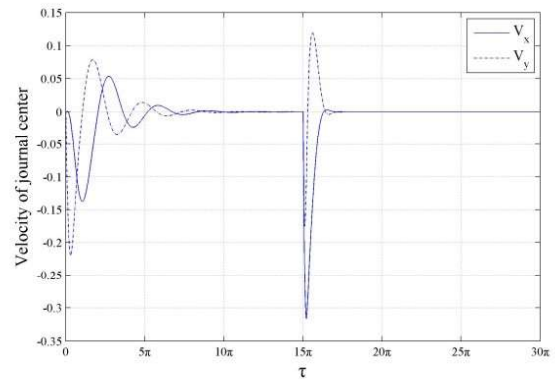
(c) Oil film components of three-axial groove bearing  
Fig. 5 Oil film components under dynamic load



(a) Journal center velocity of cylindrical bearing



(b) Journal center velocity of two-axial groove bearing



(c) Journal center velocity of three-axial groove bearing

Fig. 6 Journal center velocity under dynamic load

As shown in Figs. 4 and 5, when  $\tau < 15\pi$ , the load and oil film force are balanced, the stable position of journal center is the same as that of journal center without dynamic load, the velocity and acceleration of journal center are all zero, the oil film force and the weight of bearing are balanced. When  $\tau \geq 15\pi$ , the dynamic load begins to act on the shaft.

As shown in Fig. 3 and 4, when three kinds of journal bearings are in the static load balancing position, the  $X$  coordinates of the journal center are basically the same, but the  $Y$  coordinate is gradually away from the  $Y$  axis with the increase of the number of oil grooves. After applying dynamic load, the balance position of the journal center begins to change, moves away from the center of the bearing, and the moving distance increases with the increase of the number of oil grooves; finally, the cylindrical bearing, the two-axial groove journal bearing and the three-axial groove journal bearing are stabilized at the new balance point respectively ( $X = -0.6474, Y = -0.1324$ ), ( $X = -0.6712, Y = -0.1312$ ), ( $X = -0.8831, Y = -0.1254$ ). At the time, the  $X$  coordinates of journal center in the new balance position are gradually far away from the  $X$  axis with the increase of the number of oil grooves, and the  $Y$  coordinate of the journal center of the bearings changed from the difference obviously to basically equal. This shows that the  $X$  coordinate and  $Y$

coordinate of the journal center of three-axial groove journal bearing have the greatest change, that of the two-axial journal bearing have smaller change; the coordinates of the cylindrical bearing have the smallest change and its  $X$  coordinate remains basically unchanged.

As shown in the local enlarged drawing (1), (2) in Fig. 3, it can be seen that after the journal center is stabilized again under the dynamic load, the distance from the previous position to the new position is the shortest, and the distance from the center of the bearing is the closest, so the stability of the cylindrical bearing is the worst. Three-axial groove journal bearing has the longest journal center displacement and the farthest distance from the bearing center after the journal center is stabilized again under the dynamic load, so the three-axial groove journal bearing has the best stability. The journal center displacement of the two-axial groove journal bearing and the distance from the center of the bearing after stabilization are between that of the cylindrical bearing and the three-axial groove bearing. Therefore, the stability of the two-axial groove journal bearing is stronger than that of the cylindrical bearing and weaker than that of the three-axial groove journal bearing.

As shown in Fig. 5, after applying dynamic load, the step change of oil film component occurs. The oil film component eventually stabilizes to  $F_x=1.6085$  and  $F_y=2.4071$ , and the oil film force and load are balanced. Compared with the balanced state under static load, both the horizontal oil film component  $F_x$  and vertical oil film component  $F_y$  increase by 1.6085; the two values multiplies by  $k_m$  is equal to  $Q_x$  and  $Q_y$ , which proves again the correctness of the conclusion. As shown in Fig. 6, after applying the dynamic load, the velocity of the journal center change in step and then stabilize to zero. However, it can be found that with the increase of the number of oil grooves, the greater the change of journal center velocity after stabilization, and the faster the stabilization speed, which is consistent with the displacement analysis in Fig. 4 above. Therefore, with the increase of the number of oil grooves, the stability of the bearing is better and better. The attitude angle  $\theta$  of cylindrical bearing, two-axial groove journal bearing, three-axial groove journal bearing is 78.4419 degrees, 78.9389 degrees and 81.9197 degrees, respectively. The attitude angle of journal bearing increases with the increase of the number of bearing oil grooves after applying dynamic load.

## CONCLUSIONS

After sleeve bearing is stabilized, a dynamic load is applied, which makes the journal center oscillate and adjust again, and finally stabilizes at a new balanced position. The journal center velocity and acceleration are stabilized to zero eventually.

However, the journal center velocity and acceleration of the sleeve bearing are different with different structures. The more the number of oil grooves is, the faster the sleeve bearing journal center velocity tends to be stable. Compared with the journal center parameters under static load, the horizontal and vertical oil film components increase by the same value to counteract the dynamic load. The attitude angle will also change to a certain extent, and the change amplitude is related to the structure of sleeve bearing. The more the number of oil grooves, the greater the change amplitude of sleeve bearing, and the cylindrical bearings has the smallest change amplitude.

Under the same working condition, the change rule of the journal center position and the stability of the bearing are different when the sleeve bearing of different structures encounters dynamic load. The cylindrical bearing has the slowest stabilizing speed, the minimum eccentricity after stabilization and the worst stability. The three-axial groove journal bearing has the fastest stabilizing speed, the maximum eccentricity after stabilization and the best stability.

## ACKNOWLEDGE

This work was supported by the Fundamental Research Funds for the Central Universities, China University of Petroleum (19CX02026A).

## REFERENCES

- Cha Matthew, Kuznetsov Evgeny, Glavatskih Sergei, "A comparative linear and nonlinear dynamic analysis of compliant cylindrical journal bearings," *Mechanism and Machine Theory*, Vol. 64, pp.80-92 (2013).
- Conti R., Frilli A., Galardi E., Meli E., Nociolini D., Pugi L., Rindi A., Rossin S., "An efficient quasi-3D rotordynamic and fluid dynamic model of Tilting Pad Journal Bearing," *Tribology International*, Vol.103, pp. 449-464 (2016).
- Dong Jian, Wang Xiaojing, Zhang Jin, Xiang Xiaoqing, Nie Zhao, and Shen Jiexi, "An Experimental Research on the Vibration of Surface-Textured Journal Bearings," *Shock and Vibration*, Vol.2017, pp.1-9 (2017).
- Hakan Adatepe, Aydın Bıyıklıoğlu, Hasan Sofuoğlu, "An investigation of tribological behaviors of dynamically loaded non-grooved and micro-grooved journal bearings," *Tribology International*, Vol.58, pp.12-19 (2013).
- Hekmat M.H., Biukpour G.A. , "Numerical study of the oil whirl phenomenon in a hydrodynamic journal bearing," *Journal of the Brazilian Society of Mechanical Sciences and*

- Engineering, Vol.41, No. 5, pp.135 (2019).
- Jain Dharmendra, Sharma S.C, "Dynamic analysis of a 2-lobe geometrically imperfect journal bearing system," Proceedings of the Institution of Mechanical Engineers, Part J: Journal of Engineering Tribology, Vol. 231, No.7, pp.934-950 (2017).
- Joy Nithin M, Roy Lintu, "Determination of optimum configuration among different configurations of two-axial groove hydrodynamic bearings," Proceedings of the Institution of Mechanical Engineers, Part J: Journal of Engineering Tribology, Vol. 230, No.9, pp. 1071 – 1091 (2016).
- Lin Jaw-Ren, Li Po-Jui, Hung Tzu-Chen, Liang Long-Jin, "Nonlinear stability boundary of journal bearing systems operating with non-Newtonian couple stress fluids," Tribology International, Vol.71, pp. 114-119 (2014).
- Li Qiang, Xu Weiwei, Zhao Yue, Xing Chunlei, Jin Youhai, Zeng Shuiying, "Solution of static equilibrium position of journal bearing based on transient flow calculation," Journal of China University of Petroleum (Edition of Natural Science), Vol.39, No.2, pp.105-110 (2015).
- Li Xin Kai, "An Analysis of Journal Orbits for Nonlinear Dynamic Bearing Systems," Theoretical and Computational Fluid Dynamics, Vol.13, No.3, pp.209-230 (1999).
- Ma Jinkui, Lu Changhou, Chen Shujiang, "Simulation of Journal Centre Trajectories of Hydrodynamic Journal Bearing Under Transient Loads," Journal of Vibration, Measurement & Diagnosis, Vol. 30, No.1, pp. 6-10, 94 (2010).
- Mehrjardi M Zare, Rahmatabadi A D and Meybodi R Rashidi, "A comparative study of the preload effects on the stability performance of noncircular journal bearings using linear and nonlinear dynamic approaches," Proceedings of the Institution of Mechanical Engineers, Part J: Journal of Engineering Tribology, Vol. 230, No.7, pp.797-816 (2016).
- Meng Fanjuan, Du Yongping, "Analysis of film pressure of radial sliding bearing," Bearing, No.1, pp. 23-25, 32 (2008).
- Sharma Satish C, Kushare Prashant B, "Nonlinear transient response of rough symmetric two lobe hole entry hybrid journal bearing system," Journal of Vibration and Control, Vol.23, No.2, pp.190-219 (2017).
- Sunnegård Erik, Gustavsson Rolf, Aidanpää Jan-Olov, "Influence of cross-coupling stiffness in tilting pad journal bearings for vertical machines," International Journal of Mechanical Sciences, Vol.111-112, pp. 43-54 (2016).
- Tatsuya Miura, Tsuyoshi Inoue, Hiroshi Kano, "Nonlinear Analysis of Bifurcation Phenomenon for a Simple Flexible Rotor System Supported by a Full-Circular Journal Bearing," Journal of Vibration and Acoustics, Vol.139, No.3, pp.031012 (2017).
- Wang B, Sun Y T, Ding Q, "Free fluid-Structure interaction method for accurate nonlinear dynamic characteristics of the plain gas journal bearings," Journal of Vibration Engineering & Technologies, Vol.8, No.1, pp. 149-161 (2020).
- Wang L. L, Zeng Q L, Wang M, "Periodic Moving Track Analysis of Spiral Oil Wedge Journal Bearing under Dynamic Loading," Journal of Applied Fluid Mechanics, Vol.11, No.5, pp. 1193-1199 (2018).
- Ye Xiaoyan, Wang Jing, Zhang Desheng, Hu Lanqian, and She Xunan, "Experimental Research of Journal Orbit for Water-Lubricated Bearing," Mathematical Problems in Engineering, Vol.2016, pp.1-11 (2016).
- Zhang Z M, "Hydrodynamic lubrication theory of sliding bearing," Higher Education Press, (1986).
- Zhou Guangwu, Wang Jiaxu, Han Yanfeng, Wei Bo, Tang Baoping, Zhong Ping, "An experimental study on film pressure circumferential distribution of water-lubricated rubber bearing with multiple grooves," Tribology Transactions, Vol. 60, No.3, pp. 385 – 391 (2017).

## NOMENCLATURE

- $a_x$  the accelerations in the direction of  $x$ ,  $m/s^2$
- $a_y$  the accelerations in the direction of  $y$ ,  $m/s^2$
- $A_x$  non-dimensional accelerations in the direction of  $x$
- $A_y$  non-dimensional accelerations in the direction of  $y$
- $c$  radial clearance,  $m$
- $e$  eccentricity,  $m$
- $f_x$  component of the oil film force in the direction of  $x$
- $f_y$  component of the oil film force in the direction of  $y$
- $F_x$  non-dimensional component of the oil film



forces in the direction of  $x$

$F_y$  non-dimensional component of the oil film forces in the direction of  $y$

$g$  gravitational acceleration,  $9.8\text{m/s}^2$

$h$  oil film thickness, m

$h_g$  depth of the oil groove, ms

$H$  non-dimensional oil film thickness

$H_g$  non-dimensional depth of oil groove, m

$l$  length of the bearing, m

$m$  quality of axis, kg

$p$  oil film pressure, Pa

$P$  non-dimensional oil film pressure

$q_x$  dynamic loads acting on the rotation axis in the  $x$  direction

$q_y$  dynamic loads acting on the rotation axis in the  $y$  direction

$r$  journal radius, m

$t$  yime, s

$U$  journal rotation speed, r/min

$W$  non-dimensional loading capacity

$X$  non-dimensional displacement of the journal center in the  $x$  direction

$Y$  non-dimensional displacement of the journal center in the  $y$  direction

$\tau$  computed time,  $\tau = \omega t$

$\varphi$  circumferential angle,  $^\circ$

$\mu$  viscosity of lubricating oil

$\theta$  attitude angle,  $^\circ$

$\omega$  rotational speed of journal bearing, rad/s